Topographic variation in soil erosion and accumulation determined with meteoric ^{10}Be

Julia Marquard[1], Rolf E. Aalto[1], Timothy T. Barrows[2], Beth A. Fisher[3], Anthony K. Aufdenkampe[4,5], John O. Stone[6]

[1]Department of Geography, University of Exeter, Amory Building, Rennes Drive, Exeter, EX4 4RJ, UK, *corresponding author julia_marquard@hotmail.de

[2]School of Earth and Environmental Sciences, University of Wollongong, Wollongong, Australia and Department of Geography, University of Portsmouth, Portsmouth

[3]University of Minnesota, Dept. of Soil, Water, and Climate. 430 Borlaug Hall, 1991 Upper Buford Circle, St, Paul, MN, 55108

[4]Stroud Water Research Center, 970 Spencer Road, Avondale, PA 19311

[5]LimnoTech, 7300 Hudson Blvd, Suite 295, Oakdale, MN 55128, United States

[6]Department of Earth and Space Sciences, University of Washington, Seattle, WA 98195-1310, United States of America.

Abstract

Understanding natural soil redistribution processes is essential for measuring the anthropogenic impact on landscapes. Although meteoric ^{10}Be has been used to determine erosion processes within the Pleistocene and Holocene, fewer studies have used the isotope to investigate the transport and accumulation of the resulting sediment. Here we use meteoric ^{10}Be in hilltop and valley site soil profiles to determine sediment erosion and deposition processes in the Christina River Basin (PA, USA). The data indicate natural erosion rates of 14 to 21 mm 10^{-3} yr and soil ages of 26,000 to 57,000 years in hilltop sites. Furthermore, valley sites indicate an alteration in sediment supply due to climate change (from the Pleistocene to the Holocene) within the last 60,000 years and sediment deposition of at least 0.5–2 m during the Wisconsinan glaciation. The change in soil erosion rate was most likely induced by changes in geomorphic processes; probably solifluction and slope wash during the cold period, when ice advanced into the mid latitudes of North America. This study shows the value of using meteoric ^{10}Be to determine sediment accumulation within the Quaternary and quantifies major soil redistribution occurred under natural conditions in this region.

Keywords: meteoric ^{10}Be, geomorphology, natural soil processes, soil erosion, sediment accumulation

Introduction

Insight into natural sediment processes within agricultural areas is often difficult to achieve due to the high impact of human activity on the landscape. However, understanding and predicting natural soil movement is of fundamental importance to evaluate the magnitude of the anthropogenic impact on the Earth’s surface. This work aims to measure soil erosion and deposition during the Quaternary period in the White Clay Creek Basin located at the east coast of the USA.

The White Clay Creek Basin is a sub-basin of the Christina River Basin, which is located in the Piedmont Province of south-east Pennsylvania adjacent to the north-western part of Delaware (Figure 1). The area has not been glaciated within the last million years (Sevon and Braun, 2000). The accumulation of meteoric ^{10}Be provides information about surface processes within the last million years and allows for the assessment of long-term stability of the landscape (e.g. Willenbring and von Blanckenburg, 2010). This study uses meteoric ^{10}Be distribution with depth in soil profiles to not only determine the soil residence times and erosion rates in hilltop areas, but also to study sediment depositional processes in valley wall areas. Low relief hillslopes are expected to have significantly higher ^{10}Be concentrations than hilltop sites due to substantial ^{10}Be delivery – not only from the atmosphere – but also from sediment transport from upslope, where ^{10}Be has already accumulated. The soil profiles are also analysed for ^{210}Pb distribution with depth detect soil reallocation within the last century.

The North American east coast is an excellent location for this study because of the many well-documented records of human land use since European settlement in the 1600s. These records provide great detail on local land use and allow the identification of anthropogenically undisturbed sites. Furthermore, the records give useful information on natural, non-human impacted sediment processes within the unglaciated part of the Piedmont Province.

The Piedmont Province

The Piedmont Province is one of 6 major physiographic provinces in Pennsylvania (Figure 1; Ashley, 1933; Sevon and Braun, 2000). The geology within the Piedmont

Province was formed between about 1 billion and 600 million years ago (Ashley, 1933). The major geological unit is the Baltimore Gneiss, a Palaeozoic metasedimentary rock. Since the late Palaeozoic or early Mesozoic, the Piedmont Province experienced constant erosion with several episodes of surface uplift (Ashley, 1933; Hack, 1982). As a consequence, the landscape is marked by rounded hills with deep soils due to well-weathered bedrock (Ashley, 1933; Newbold et al., 1997; Barnes and Sevon, 2002).

Glacial evidence in the form of eskers, moraines, kettles, boulders and valleys are found in north-east and north-west Pennsylvania (Ashley, 1933; Braun, 2004). Three glacial advances have been documented in north-eastern and north-western Pennsylvania within the last million years: pre-Illinoian advance (> 770,000 years), late Illinoian advance (132,000–198,000 years) and Wisconsinan advance (17,000–22,000 years) (Sevon and Braun, 2000) (Figure 1). The late Illinoian and pre-Illinoian glacial advance extended 10–30 km further south than the Wisconsinan glaciation within Pennsylvania (Clark and Ciolkosz, 1988). The Piedmont Province has not been glaciated. However, surface temperature ~12°C lower than present created a periglacial climate in most parts of Pennsylvania (Nelson, 2007). Clark and Ciolkosz (1988) reviewed evidence for a periglacial environment during the Wisconsinan glaciation (see Figure 1) south of the glacial border. Evidence of a periglacial environment can be found in the form of blockfields and blockstreams between ~170–570 m in elevation and as sorted patterned ground (at 701-975 m elevation; Clark, 1968), both likely to have formed under permafrost, but at a higher elevation than the Piedmont area (100–200 m in elevation). Periglacial blockfields have been documented in 6 main groups in the highlands (Nelson, 2007 and references therein) including, for example, the Blue Rocks blockfield (Hamburg, PA, USA) 70 km north of the study site. This suggests that the ground surface in the Piedmont Province may have experienced multiple cycles of freezing and thawing. Furthermore, gravitational mass movements in the form of periglacial solifluction occurred (Matsuoka, 2001; Barnes and Sevon, 2002; Zepp, 2011). In particular, steep slopes (> 10 %) resulted in higher rates of soil erosion compared to gentle slopes in the highlands during the colder periods in the Pleistocene (Ciolkosz et al., 1989).

Due to the lower altitude and relief in the Piedmont area, periglacial effects can be expected to be less intense than in the highlands (Ciolkosz et al., 1989). Nelson estimated the elevation of the 13°C isotherm at circa 100 m altitude in the wider study area and found almost all periglacial landforms lay above this altitude. The 13°C isotherm approximates the treeline (Cogbill and White, 1991), a major geomorphological boundary. Ciolkosz et al. (1989) observed ridge and valley areas in Pennsylvania to be substantially covered by footslope colluvium (27 % of the ridge and valley areas). However, a further quantification of sediment processes caused by temperature decrease during the Pleistocene, which resulted in multiple periglacial episodes within the Piedmont Province, has not been conducted.

All of these observations suggest that different processes have operated on soils in the Piedmont Province of Pennsylvania through time. In this study, we use ^{10}Be depth and ^{210}Pb distribution to quantify soil erosion processes in the Piedmont Province. Besides determining erosion rates in the study area, this paper further tests the ability to determine rates of sediment deposition using meteoric ^{10}Be in soils.

Meteoric ^{10}Be and ^{210}Pb in soil profiles

Meteoric ^{10}Be is a naturally occurring fallout radionuclide with a relatively long half-life of 1.39 × 10^6 years (Chmeleff et al., 2009). It is produced in the atmosphere mostly by nuclear spallation of ^{16}O. Meteoric ^{10}Be is delivered to the soil surface by wet or dry deposition, where it infiltrates with rain and adsorbs to soil particle surfaces

(Willenbring and von Blanckenburg, 2010). This nuclide has been used to determine ^{10}Be residence time (Fifield et al., 2010), soil age (Egli et al., 2010; Ebert et al., 2012), rates of soil production and erosion (Fifield et al., 2010, Dannhaus et al., 2017, Waroszewski et al., 2018), hillslope processes (Jungers et al., 2009; West et al., 2013, 2014), sediment transport/tracing (Belmont et al., 2011) and recording of the magnetic field strength (Frank et al, 1997).

Meteoric ^{10}Be accumulation within a soil profile records information about soil redistribution processes within an area of interest over time scales up to 10^7 years (e.g. Jungers et al. 2009; Willenbring and von Blanckenburg, 2010; Graly et al., 2010 and 2011). In turn, meteoric ^{10}Be accumulation within a soil depends on regolith characteristics (physical and chemical) and on ^{10}Be supply (sediment deposition, atmospheric delivery, dust). Meteoric ^{10}Be distribution with depth is influenced by different soil characteristics (Graly et al., 2010; Schoonejans et al., 2017). These characteristics include, among others, grain size and pH (Willenbring and von Blanckenburg, 2010). In addition, a correlation of ^{10}Be to dithionite-citrate extractable aluminium and iron is observed (Barg et al., 1997; Graly et al., 2010). Soil profiles from sites that have not been under anthropogenic influence are expected to differ from anthropogenic sites due to a change in soil characteristics (both physical and chemical). In addition, the ^{10}Be profiles in sediment depositional sites (e.g. valleys) differ from predominantly erosional sites (e.g. hilltops). A comparison of chemical soil characteristics and their environmental background as well as meteoric ^{10}Be distribution with depth can give valuable information about the sediment movement as well as processes within the sample area.

Graly et al. (2010) compared 27 studies working with meteoric ^{10}Be in soil profiles, which all showed the highest ^{10}Be concentration in the upper 1.5 m of the soil surface. Furthermore, the authors recognised two general shapes of ^{10}Be distribution in soil: ‘bulge’ and ‘declining’ type profile. In the bulge type profile, the highest ^{10}Be concentrations are found within the B-horizons (two to three times higher) with a subsequent decline in ^{10}Be concentration. In comparison, the decline type profile has peak concentrations at the soil surface and a decrease in ^{10}Be concentration with depth. These decline type profiles are usually found in actively eroding hillslopes or young soils (Graly et al., 2010). Generally, no significant meteoric ^{10}Be is present in soil C-horizons (Graly et al., 2010; West et al., 2013).

The total ^{10}Be accumulation can be determined by calculating the inventory *N* [atoms cm^{-2}] in the soil profile (Pavich et al., 1985; Willenbring and von Blanckenburg, 2010; Graly et al., 2010; West et al., 2013):

$$N = \sum n \times \rho_s \times l \qquad \text{Equation 1}$$

where n [atoms g^{-1}] is the ^{10}Be concentration, ρ_s [g cm^{-3}] bulk density and l [cm] the sample length of each interval. This is true for all shapes of ^{10}Be profiles (Lal et al., 2012) and assumes no inherited ^{10}Be from bedrock material (Pavich et al., 1985). Equation 1 will give a minimum inventory, if sampling of the entire ^{10}Be profile is not assured (Fifield et al., 2010). Potential ^{10}Be loss could be related to desorption during changing pH and redox conditions (Pavich et al., 1985). Furthermore, the time required for ^{10}Be accumulation (*t*) can be determined using *N*, where ^{10}Be delivery equals ^{10}Be removal (Graly et al., 2010; West et al., 2013). For a site with no ^{10}Be deposition apart from atmospheric ^{10}Be deposition, *t* can be calculated as follows:

$$t = \left(\frac{-1}{\lambda}\right)\log_e\left(1 - \left(\lambda \times \frac{N}{q}\right)\right) \qquad \text{Equation 2}$$

where λ is the decay constant of ^{10}Be 5×10^{-7} year^{-1} (Korschinek et al., 2010), q is the ^{10}Be fallout flux (or delivery rate) to the soil surface that is assumed to be constant if averaged over long timescales (Graly et al., 2010). Calculations by Willenbring and von Blanckenburg (2010) based on two models by Field et al. (2006) and Heikkillä (2007) give an approximate delivery rate of 1.2×10^6 ^{10}Be atoms cm^{-2} year^{-1} to the Christina River Basin.

Equation 3 determines the erosion rate E [g cm^{-2} year^{-1}] (Graly et al., 2010):

$$E = \frac{(q - \lambda N)}{C_v} \qquad \text{Equation 3}$$

where C_v is the ^{10}Be concentration [atoms g^{-1}] of the top sample assuming this is the eroding material. Soil erosion rates can be determined for the hilltop profiles following Pavich et al. (1985), Brown et al. (1988), Jungers et al. (2009), Graly et al. (2010), West et al. (2013) and others. Determination of soil age is possible if sediment erosion can be excluded as a possibility and the soil is relatively young, as for example, in a recently deglaciated area (Balco, 2004; Ebert et al., 2012). For very old soils, which are affected by soil erosion, Equation 2 gives a soil residence time (Bacon et al., 2012; West et al., 2013). Furthermore, if assuming steady state, soil erosion rate can be determined using the ^{10}Be inventory, i.e. Equation 3 (Graly et al., 2010). Steady state assumes equal amounts of ^{10}Be removed by soil erosion and ^{10}Be supplied by fallout (Graly et al., 2010). The utility of ^{10}Be in evaluating the erosion rates in the Piedmont area in slowly eroding soils has previously been demonstrated by Pavich et al. (1985), Brown et al. (1988), Stanford et al. (2000), Jungers et al. (2009), Bacon et al. (2012) and West et al. (2013).

^{210}Pb is a naturally occurring fallout radionuclide that derives from the decay of ^{226}Ra in the ^{238}U chain (He and Walling, 1997; Mabit et al., 2008; Persson and Holm, 2011). It deposits via wet or dry deposition and binds tightly to sediment particles, even in acidic conditions (Simms, 1988; Davies, 1992). The natural origin of ^{210}Pb results in relatively constant fallout rate through time. The half-life of ^{210}Pb is 22.3 years, much shorter than the half-life of ^{10}Be, and is convenient to detect soil redistribution within the last decade.

^{210}Pb activity is highest at the top of an undisturbed profile and decrease monotonically with depth (He and Walling, 1997). However, ^{210}Pb activity does not usually reach zero due to decay of uranium in soil minerals ('supported ^{210}Pb'; Aalto and Nittrouer, 2012). This background ^{210}Pb concentration can be estimated by comparing different undisturbed profiles and is usually found between 10–20 cm depth, although this can vary depending on soil characteristics (e.g. He and Walling, 1997; Perreault et al., 2012 and Mabit et al., 2008).

^{210}Pb has been used widely to determine soil redistribution in various study areas (e.g. He and Walling, 1997; Goodbred and Kuehl, 1998; Aalto et al., 2003; Resner et al., 2011; Aalto and Nittrouer, 2012) and is used here to detect soil redistribution within the last century in order to help understanding ^{10}Be distribution with depth.

Methodology

Sample collection and analysis

In total, five soil profiles were collected from different environments using a push corer and an auger. Profiles were collected from the following hillslope positions: hilltop, slope and lowland as well as forested or agricultural areas. Profile depths varied from 204–310 cm, where the sampling depth depended on the density of the regolith (especially grain size). Four of the profiles came from potentially undisturbed sites (with minimum anthropogenic influence) and one soil profile was collected from an agricultural field. At hilltop sites (Penn Oak, Weather Station), the push corer was able to sample the entire regolith thickness into saprolite. Nine to ten even distributed samples (2 cm homogenised depth intervals) were taken from these profiles (see Table 2), avoiding sand lenses due to grain size dependency and less ^{10}Be attached to sand particles (Willenbring and von Blanckenburg, 2010). Valley site profiles contain depth increments of varying size with seven samples per profile, also evenly distributed with depth to gain a representative insight of the ^{10}Be distribution. The clay concentration was measured for the same depth intervals as ^{10}Be. Prior to ^{10}Be analysis, soil profiles were analysed for ^{210}Pb in the facilities of the University of Exeter (UK) in order to determine major soil reallocation within the last century. ^{210}Pb was determined by measuring ^{210}Po (granddaughter nuclide of ^{210}Pb), since these radionuclides should be in secular equilibrium due to their mutual relationship (Bonczik, 2013). Adsorbed ^{210}Po was extracted from the sediment by conducting a sequential leaching extraction developed by Aalto and Nittrouer (2012). Subsequently, ^{210}Po was auto deposited onto silver planchets and counted for ^{210}Po on the alpha spectrometer (Ortec Ultra-AS).

Grain size was measured using the SediGraph® in the laboratories of the University of Exeter (UK). Citrate-dithionite extractable iron and aluminium measurements were conducted in the laboratories of the University of Exeter (UK) as well as the University of Minnesota (USA) after methods from Blakemore et al. (1987). 10Be was extracted from the soil utilising the rapid fusion method of Stone (1998) in the Cosmogenic Nuclide Chemistry Laboratory of the University of Washington (USA). 10Be analysis was undertaken by measuring ^{10}Be/^{9}Be by accelerator mass spectrometry at Lawrence Livermore National Laboratory. Analytical error and 10Be background concentration is detected on the basis of three blank measurements. $^{10}Be/^{9}Be$ measurements were normalised to the 07KNSTD3110 standard. Propagation of uncertainty was calculated by taking the square root of the sum of the squared different relative errors as the error of the balance (1 %) and the error of the ^{10}Be measurement (between 0.6 and 2.3 %).

Study sites

Sampling was mainly focused within a single watershed, with most of the soil profiles in the northern part of the White Clay Creek basin (one profile was taken just over the drainage divide in the Red Clay Creek watershed; Figure 2 (A) and (B)). The profiles are referred to as Weather Station, Ag-Field, Penn Oak, Bluebell Meadow and Wy-Wood, based on their locations (Figure 2 (A)-(C)). Figure 2C provides an insight into the topography of each sample site; quantitative measures of the topography are listed in Table 1. The profiles Weather Station and Penn Oak are collected from hilltop sites, the Ag-Field profile from a slope area and the Bluebell Meadow and Wy-Wood from valley sites.

Hilltop sites

The Weather Station sample site is situated in the White Clay Creek watershed on a hilltop at the edge of an open field within a line of trees (Figure 2). The soil profile was sampled underneath the bottom of an old oak tree that had recently toppled, exposing bare soil previously directly under its trunk. The soil is from the Glenelg/Glenville Series, which are ultisols and moderately to well-drained soils. The saprolite underneath is Setters Quartzite, which is part of the Glenarm Group and consists of 80% to 90% of quartz with microcline, muscovite, and biotite (Blackmer, 2005). According to its size, the tree was probably at least three hundred years old, and fell in natural circumstances in the past few years. Due to the fact that the profile was sampled from soil previously located directly underneath the tree, no human induced erosion is expected at this site.

The soil profile Penn Oak soil profile originates from a hilltop site in the north-east of the White Clay Creek watershed (Figure 2C). The sample site is close to the town's Friends meeting house, with approximately 5 m distance to an old oak tree that is well over 300 years old according to tree rings counted in the field. Since this place is of religious value for the community for many generations no major human induced sediment redistribution is assumed. The soil of this profile is from the Parker Series, an inceptisol, which is marked by well-drained conditions. The saprolite beneath is from amphibolite gneiss. Amphibolite Gneiss is part of the Baltimore Gneiss that is major geological unit of the study site and is a plagioclase-hornblende-quartz-biotite with local orthopyroxene, clinopyroxene, potassium feldspar and garnet (Blackmer, 2005). Due to its position on hilltops with moderate slope angles (Table 1), the Penn Oak and Weather Station sample sites are assumed to be constantly eroding and have insignificant soil accumulation.

Valley sites

The valley site profiles are sampled in concave hollows located either on the valley floor or as clear breaks in slope that would tend to collect sediment transported from upslope. The Ag-Field profile was collected in an agriculture field within a sloped area (Figure 2C; Table 1) and is expected to undergo substantial soil erosion as well as sediment deposition from upslope. Again, it is in the watershed of White Clay Creek. The 'no till' technique is practised within the field for cultivation purposes, which involves soil loosening within a maximum of 45 cm depth with the help of a deep, L-shaped bar (personal communication with farmers). Mushroom compost is the primary soil conditioner and is applied every three years since the year 2000. The profile is like the Weather Station site with a Glenelg/Glenville soil over a Setters Quartzite-derived saprolite.

The Bluebell Meadow profile is the only soil profile taken in the neighbouring watershed Red Clay Creek, just on the drainage divide White Clay Creek (Figure 2). The sample site is on a strip of woodland that acts as a field boundary located on relatively level land (5 %; Table 1). Similar to the Penn Oak profile, the soil is from the Parker series, a well-drained inceptisol and saprolite is formed from underlying amphibolite gneiss. Immediately adjacent to the sample location sits an ancient oak tree (> 300 years), which implies a relatively undisturbed site. 10 m distant, relicts of an ancient farm track can be observed, although this lies across an equally derelict fence line that has not been in use for a long time. Coring was difficult at this site, in that impenetrable bedrock was encountered multiple times at 70–90 cm depth.

The Wy-Wood study site in Weymouth Woodhole is situated in a forest in a depressed area. The area is assumed to have been forested since and before the European Settlement. This is indicated by maps (from 1937), which show abundant full-grown trees, suggesting minimal anthropogenic influence on sediment reallocation. The profile was sampled by using a push corer for the first few metres. Deeper samples were sampled with an auger. The soil is from the Glenville Series and therefore a moderately drained ultisol. The saprolite underneath is from Doe Run Schist (Glenarm Wissahickon formation), which is a garnet-staurolite-kyanite pelitic schist with abundant biotite and muscovite (Blackmer, 2005).

The Wy-Wood and Bluebell profile are expected to show only minor soil erosion but significant soil deposition due to their position on valley floors with only a shallow slope (Figure 2C, Table 1).

Results

Hilltop profiles (Penn Oak, Weather Station)

The hilltop profiles generally show a declining meteoric ^{10}Be distribution with depth (Figure 3; Table 2). The majority of the ^{10}Be inventory is in the first 50–100 cm of the profile. There is no significant ^{10}Be below 1.5 m. For both profiles, the clay concentration roughly follows the trend of ^{10}Be. ^{210}Pb activity generally declines in the Weather Station profile. However, for the Penn Oak profile, increased ^{210}Pb activity can be found even at greater depth. Further details for the different soil profiles set in relation with the additional data are described below.

Penn Oak:

The first 50 cm of the Penn Oak profile shows very high ^{10}Be concentrations with little variation. This trend is also observed in the clay concentration. Below 50 cm, ^{10}Be concentration decreases. In addition, clay is enriched in the lower horizon where ^{10}Be has preferentially accumulated creating a bulge profile (Graly et al., 2010). ^{210}Pb activity generally declines within the first 20 centimetres (Figure 6B) – whereas there is relatively high ^{210}Pb at 10 cm – and increases again between 20 cm and 70 cm following by another decrease of ^{210}Pb activity. Highest ^{210}Pb concentrations are at 70 cm with an activity of about 84 mBq/g.

Weather Station:

The tree on the sample site fell over in 2005 or 2006 according both to local residents and ^{210}Pb dating of the meteoric cap (high concentration at the top with a constant decrease with depth; Aalto and Nittrouer, 2012). ^{10}Be concentration sharply declines with depth. ^{210}Pb activities also decrease gradually with depth (Figure 6D), whereas maximum activities of about 44 mBq/g are much lower than in all other profiles. Below 4 cm there is a constant ^{210}Pb activity of about 13 mBq/g. Importantly, the base of the Oak contained no taproot, so there was very little tree throw soil disturbance when it fell over.

pH values were measured for the first 70 cm of the profile near the weather station and identify the profile as slightly acidic with pH 5.0 (Table 2). No pH was measured for the Penn Oak profile.

Valley site profiles (Bluebell Meadow, Ag-Field, Wy-Wood)

The ^{10}Be concentration with depth in the valley site profiles is very different to the profiles of hilltop areas (Figure 4 and 5; Table 2). The ^{10}Be concentrations are, in general, very high throughout all profiles and maximum concentrations are more than double those of profiles in hilltop areas. A comparison of ^{10}Be concentration to additional soil data (pH, clay and dithionite extractable Fe and Al, if available) does not show any correlation. For all valley site profiles a general declining ^{210}Pb activity can be observed with the exception of the Ag-Field profile. Each profile is described in detail below.

<u>Bluebell Meadow:</u>

^{10}Be concentrations in the soil profile of Blue Meadow display a high variability, potentially reflecting the unusual sampling conditions (Figure 4). The maximum ^{10}Be concentration is at 60 cm with a gradual decreasing trend below that depth.

Generally, the ^{10}Be inventory is an order of magnitude higher in the profiles sited on valley hollows compared to the profiles of hilltops. Also, maximum concentrations are much higher in valley hollow profiles. The ^{210}Pb with depth shows high concentration at the top and a decrease with depth. The ^{210}Pb activity is relatively constant with about 18 mBq/g at depths greater than 20 cm (Figure 6A). The first 50 cm display a moderate and constant clay concentration, but clay increases below this depth.

<u>Ag-Field:</u>

The Ag-Field profile is the only profile that is highly disturbed due to anthropogenic impact (Figure 5 (A)). This profile displays very high ^{10}Be concentration, much higher than all other profiles sampled for this study, with no gradient with depth. The clay concentration is especially high in the first 70 cm, presumably due to agricultural practices in the form of soil loosening that lead to clay migration and clay accumulation in deeper horizons (Scheffer and Schachtschabel, 2010). ^{210}Pb activities slightly decline within the first 13 cm (maximum: 48 mg/g) and then stay relatively constant with around 25 mBq/g until the bottom of the profile at 60 cm. The clay concentration decreases below this depth and remains relatively constant throughout the lower part of the profile. Fe_2O_3 concentrations are constant with depth, with only a slight increasing trend towards the bottom of the profile, whereas Al_2O_3 is quite variable. The agricultural profile shows the highest pH level found within all profiles in this study, with slightly alkaline conditions (pH 7.8). Overall, there is a decreasing trend in pH towards the bottom of the profile (lowest pH 5.3).

Wy-Wood:

This profile has very high ^{10}Be concentrations at the top of the profile and decreases monotonically from 20 cm to about 100 cm where it rises again gradually with increasing depth to the bottom of the core (Figure 5 (B)). ^{210}Pb analyses show high ^{210}Pb activities at the top and a gradual decrease with depth, with maximum activities of 400 mBq/g (Figure 6C). Below 12 cm ^{210}Pb activities are relatively constant with about 15 mBq/g. The clay concentration within this profile varies within the top 70 cm, decreasing with depth. Measurements of pH value indicate acidic soil (pH 4–5), with a slight increase towards the bottom of the profile.

Discussion

Hilltops

Both hilltop soil profiles are sited in relatively undisturbed areas. Hence, the meteoric ^{10}Be inventory or residence time reflects natural conditions within the area. The correlation of clay and ^{10}Be concentration could be a sign of illuviation of clay with adsorbed ^{10}Be, or ^{10}Be is simply adsorbed to previously existing clay. It must be considered that the hilltop profiles are characterised by different lithologies. This can possibly have an influence on ^{10}Be adsorption and therefore on the ^{10}Be distribution with depth.

It is well known that trees and their roots play an important role on soil formation and mixing locally (Brantley et al., 2017 and refs therein). However, soil mixing is assumed to be minor at the Weather Station sample site, since the ^{210}Pb profile suggests no major sediment redistribution within the last 100 years. Furthermore, ^{10}Be data indicates no sediment redistribution over the longer timescale at the Weather Station sample site, indicating limited bioturbation.

Anthropogenic disturbances and bioturbation are more likely at the Penn Oak sample site. Subsequently we found that additional soil was added to the surface to protect the roots of the tree given its special value for the residents (personal communication with Dr. D. Newbold, Stroud Research Centre). Furthermore, this site has always had public access, for example horses and vehicles parking near the meeting house, potentially leading to sediment redistribution at the site. This would have the effect of shifting the maximum ^{10}Be concentration deeper in the profile. The slight increase of ^{10}Be at 50 cm is suggestive of this. The assumption of soil emplacement is supported by ^{210}Pb data, which records disturbances in the top 10 cm only within the last 100 years (Figure 6 (B)). The increase in ^{210}Pb concentration at 60 cm can be related to gneiss, a uranium bearing rock type (Degens et al., 1957). Hence, uranium decays to ^{210}Pb and accumulates in the profile. Despite the slight acidity recorded for the profile near the Weather Station and the unknown pH of the soil within the Penn Oak profile, mobility of meteoric ^{10}Be due to pH dissolution through the profiles appears unlikely. This is indicated by the fact that (i) ^{10}Be concentrations at the bottom of both profiles are 4 % or less than at the soil surface and (ii) by the general decrease of ^{10}Be with depth, which both suggest that most of the ^{10}Be inventory has been sampled (cf. Fifield et al., 2010). Maximum concentrations fall in the range of other ^{10}Be studies (e.g., Graly et al., 2010), but are relatively low for studies within the Piedmont Province (Pavich et al., 1985; Brown et al., 1988; Stanford et al., 2000; Jungers et al., 2009; Bacon et al., 2012; West et al., 2013).

The ^{10}Be inventory for the Penn Oak profile determined with Equation 1 of 6.70 ± 0.11 × 10^{10} atoms cm^{-2} indicates an accumulation period of 57,000 ± 900 years (Table 2). If the first 50 cm are not included in the determination, due to the possible emplacement of soil to protect the tree roots, a ^{10}Be inventory of 4.32 ± 0.08 × 10^{10} atoms cm^{-2} is determined, which in turn is 36,000 ± 700 years. The Weather Station sample site has a ^{10}Be inventory of 3.08 ± 0.05 × 10^{10} atoms cm^{-2} indicating a ^{10}Be accumulation time of 26,000 ± 400 years (Table 2). The differences in ^{10}Be within the two hilltop profiles are presumably associated with differences in lithology (soil/ rock type) or/and the local topographic conditions given that the Penn Oak sample site is situated on flatter area and may have received soil from upslope (Figure 2 (C)).

Calculated ^{10}Be inventories and residence times are an order of magnitude lower than reported for other sites in the eastern US (Graly et al., 2010). Our data suggest that ^{10}Be has accumulated during the late Pleistocene, and certainly during the last glacial period (Sevon and Braun, 2000). The lower ^{10}Be inventory compared to other studies in the Piedmont Province and is probably the result of the site location on hilltop sites where constant erosion occurs. A further factor reducing the ^{10}Be

inventory could be the sampling method used for this study. Only 2 cm intervals at different depths within the profiles were taken, rather than choosing larger intervals with bulk sampling of the entire profiles, as conducted in other studies (Graly et al., 2010). Consequently, layers with very high ^{10}Be concentration might have been missed, resulting in a lower calculated inventory. However, sand lenses with presumably less ^{10}Be attached (grain size effect; Willenbring and von Blanckenburg, 2010) were avoided that could possibly influence the ^{10}Be inventory. To reduce the sampling effect, more samples were taken within the first 50 cm of the profile where higher ^{10}Be concentration is expected as observed by Graly et al. (2010). At greater depth a sample was taken approximately every 50 cm.

No ^{10}Be elution into the saprolite is expected, so we assume sampling of the entire ^{10}Be profile. Assuming steady state soil erosion can be determined using Equation 3. First, the ^{10}Be concentration of the eroding material (C_v) has to be assumed in order to calculate erosion rates using this approach. The ^{10}Be inventory of the surface samples (taken at 10-12 cm of depth) within the hilltop profiles is assumed to be representative for the eroding material, which is then deposited on valley sites. For the Penn Oak profile, scenarios with both a declining and also a bulge ^{10}Be profile are considered. The resulting erosion rates were 22 ± 0.28 mm 10^{-3} yr (≙3.12 ± 0.04 10^{-3} g cm^{-2} year^{-1}) assuming a bulge profile and 14 ± 0.28 mm 10^{-3} yr (≙2.53 ± 0.05 10^{-3} g cm^{-2} year^{-1}) respectively considering a declining profile within the Penn Oak sample site and neglecting the first 50 cm due to possible soil emplacement (see discussion above). The Weather Station site has an erosion rate 17 ± 0.25 mm 10^{-3} yr (≙2.36 ± 0.04 10^{-3} g cm^{-2} year^{-1}). Soil movement (e.g. caused by solifluction) would likely be limited within these two sample sites due to their flat topography – removal of ^{10}Be is solely driven by sediment erosion since ^{10}Be dissolution is thought to be minor (see above). Soil production rates and sediment removal are in equilibrium within the Piedmont area according to Pavich et al. (1985), and making that assumption here implies a soil production rate of around 18 ± 0.27 mm 10^{-3} yr (average of the erosion rates determined for the two hilltop sites). These rates are slightly higher than those found for the Piedmont area by Stanford et al. (2000) (10 mm 10^{-3} yr based on meteoric ^{10}Be) or Reusser et al. (2015) (8 mm 10^{-3} yr based on in situ ^{10}Be), but lower in comparison to the Appalachian Mountains with about ~43 mm 10^{-3} yr (West et al., 2013; Ma et al., 2013). Furthermore, the erosion rate is relatively low compared to mountainous regions such as the Alps with 30 mm 10^{-3} yr (Schaller et al., 2002), the Himalayan mountain belt 1200 mm 10^{-3} yr (Vance et al., 2003) and the southern Alps of New Zealand with even 2500 mm 10^{-3} yr (Larsen et al., 2014). Higher erosion rates are related to the higher slopes in these tectonically active areas (Leser, 1977), thinning soils and thereby increasing soil production rates. In contrast, the landscape in the Piedmont Province is tectonically quiescent since the late Paleozoic or early Mesozoic (Hack, 1982). This has resulted in a smooth, rounded landscape (Barnes and Sevon, 2002) covered with relatively thick soils hence no major erosion is expected without the influences of anthropogenic impact.

Valley sites

The ^{10}Be soil profiles sampled in the valleys are more complex than the hilltop profiles, in that the concentrations do not simply decline with depth. This is because the sample sites have received substantial episodic sediment contribution due to their location on foot slopes or other mid-slope breaks. These additions from upslope greatly increase the total inventory, which consequently includes more than just meteoric ^{10}Be fallout content directly on the site.

^{210}Pb indicates negligible soil redistribution within the last century at the Blue Meadow sample site due to an undisturbed declining profile (He and Walling, 1997). However, the increase of clay as well as Fe and Al towards the bottom of the profile may suggest soil leaching during pedogenesis, which also has consequences for the ^{10}Be distribution with depth. This interpretation is also supported by relatively low pH values (pH 4–4.5). Sampling of the profile was difficult due to large blocks of quartzite at depth. These unconformities in the soil structure probably influenced clay movement within the soil profile, especially in regard to the deeper samples. Furthermore, due to the proximity to an historic farm path nearby this sample site, anthropogenic disturbance within the first few centimetres of the soil profile is a possibility.

Within the Ag-Field profile ^{210}Pb analysis reflects the agricultural nature of the soil within the last century and records soil mixing up to a depth of 40 cm (He and Walling 1997; Figure 6 (E)). The high pH presumably reflects the application of lime by the farmer for agricultural purposes.

The Wy-Wood profile shows no soil mixing within the last century according to the ^{210}Pb activity. Although ^{10}Be generally decreases with depth, concentrations are much higher than for the hilltop profiles and suggest substantial sediment supply within the timing of ^{10}Be accumulation (Table 2),

The increased maximum ^{10}Be concentration in the valley site profiles compared to the hilltop profiles are presumably caused by net sediment accumulation that occurred over time in the lower areas. However, in all profiles sited on valley hollows, the ^{10}Be concentration is relatively higher at the bottom. Therefore, it is most likely that the entire inventory has not been sampled and ^{10}Be exists at even greater depths than the current profiles have been sampled. For this reason, ^{10}Be inventories determined for valley hollow profiles probably underestimate the total inventory.

Sediment that is deposited at the valley sites comes from sediment erosion in the hilltop soils that supply ‘inherited’ ^{10}Be in addition to ^{10}Be accumulated at the site. To assess accumulation times, the ^{10}Be concentration of the delivered material has to be known, which may be estimated from the hilltop profiles. The Penn Oak and Weather Station profiles have similar surface concentrations of 4.7 and 5.0 × 10^8 atoms g^{-1}, which are the maximum values for the profiles. This ignores the first 50 cm of the Penn Oak profile that is presumably recently added (see above). Since sediment erosion and production is assumed to be in equilibrium, and the hilltop sites were selected for the minimal anthropogenic influence, the concentration of 4.84 ± 0.08 atoms g^{-1} is an appropriate value to represent the ^{10}Be ‘inherited’ concentration through time. However, ‘steady state’ erosion during the glacial period is unlikely due to the short age of the soil. Therefore, modern topsoil has presumably higher ^{10}Be concentration than during glacial periods. Radioactive decay of ^{10}Be can be neglected due to the short period of observation, considering a ^{10}Be residence time in soil of 9.73 million years (Graly et al., 2010). The inherited ^{10}Be content $^{10}Be_{in}$ then has to be subtracted from the ^{10}Be content analysed within the valley floor profile $^{10}Be_t$ in order to calculate the amount of ^{10}Be that accumulated with time ($^{10}Be_a$).

$$^{10}Be_a = {}^{10}Be_t - {}^{10}Be_{in} \qquad \text{Equation 4}$$

This further enables an identification of changes in ^{10}Be accumulation and therefore changes in sediment deposition. A change in sediment deposition occurs whenever there is an increase in ^{10}Be concentration with depth and allows the determination of ‘sediment packages’ with a certain inventory ($^{10}Be_t$): A constant supply of ^{10}Be fallout and soil deposition (with $^{10}Be_{in}$ attached) to a depositional site has a constant concentration with depth as a consequence. If soil deposition comes to a halt, only

^{10}Be supply by fallout occurs, ^{10}Be accumulates and a meteoric cap (high concentration at the top and decrease with depth) can evolve.

Using Equation 4 for the different 'sediment packages' and substituting into Equation 2, gives the period of ^{10}Be accumulation (see Figure 4 and 5 for results). The period of accumulation is assumed to be minimum due to the use of ^{10}Be concentration of modern topsoil for 'inherited' ^{10}Be, since topsoil from glacial period is expected to have a lower ^{10}Be concentration (see above). There is much uncertainty within the Bluebell Meadow profile and soil redistribution is suggested by ^{10}Be concentration with depth. However, all three profiles suggest substantial ^{10}Be accumulation ages for 12,000 to >78,000 years, where 0.5–2 m of sediment is deposited, which results in an average accumulation rate of 125 cm per 39,000 years. Much of this accumulation appears to have occurred during the Wisconsinan glaciation, dated 17,000–20,000 years ago (Sevon and Braun, 2000). During this period, the periglacial area may have extended to the Piedmont area with permafrost on hilltop areas, enhancing sediment erosion due to continuous cycles of soil freezing and thawing (cf. Zepp, 2011). Hence, solifluction processes could have led to major soil mobilisation and sediment deposition in the valleys. During the present interglacial period, the rate of sediment deposition has decreased because of increased vegetation cover and only $^{10}Be_a$ accumulates due to atmospheric fallout.

Sediment deposition in periglacial environments of 0.5–2 m during one glaciation (80,000 years) is likely (Matsuoka, 2001). Sediment erosion is assumed to be minor on the sample site of the Wy-Wood and the Bluebell profile during the last 80,000 years due to low relief energy (Figure 2 (C)). However, the sample site of the Ag-Field is situated on a sloped area (Figure 2 (C)) and therefore sediment erosion is likely, which implies a higher soil accumulation rate than detected. Uncertainties due to spatially varying lithology, climate variations as well as human interference and bioturbation must also be considered as stressed for the hilltop profiles. However, considering the study area is relatively flat, this sediment accumulation may be realistic (Clark and Ciolkosz, 1988).

Conclusions

This study shows that an analysis of ^{10}Be distribution in soil profiles provides insight into natural soil mobilisation processes of an area over millennial time scales. Quantification of these natural processes is a necessary step towards evaluating post-settlement anthropogenic impacts on the landscape.^{10}Be distribution with depth in undisturbed settings allows determination of natural soil erosion and redeposition within the Quaternary. Moreover, knowing the ^{10}Be inventory in eroded hilltop soils allows determination of timing of sediment deposition in valley hollow sites, if:

- incoming material has a relatively constant ^{10}Be activity, which can be assessed using hilltop profiles,
- vertical sediment mixing within the sample site is minimal,
- ^{10}Be pH dissolution is relatively minor.

Investigations of the anthropogenic history of the sample sites are a requirement before sampling to minimise the influence of human impact on soil redistribution and ensure that natural conditions are documented. Subsequently, ^{10}Be distribution can be compared with the last million years of soil formation and landscape evolution. Long-term (>10^3 years) changes in sediment supply through glacial and interglacial periods , can be detected and the timing of soil accumulation determined.

The following main conclusions can be drawn concerning the soil dynamics in the Piedmont Province:

- The hilltop soils formed in the last 26,000–57,000 years and likely experienced constant erosion.

- Soil erosion and production rates are 14–21 mm 10^{-3} yr; classifying these sites as slowly eroding soils (Graly et al., 2010).
- Valley hollow profiles display changes in sediment supply to the sites, which can be related to long-term climate change since the last glacial period.
- Sediment deposition of at least 0.5–2 m occurred during the Wisconsinan glacial period.

Acknowledgements

The authors are grateful for intellectual and field support from Diana Karwan and Kyungsoo Yoo. The University of Washington and Lawrence Livermore Laboratory provided facilities for the ^{10}Be analyses, with Zachary Ploskey and Perry Spector providing lab assistance. Project funding was provided by the Christina River Basin Critical Zone Observatory (NSF EAR 0724971), with PhD support for J. Marquard provided by Erhart Muller and the University of Exeter.

References

Aalto RE, Maurice –Bourgoin L, Dunne T, Montgomery DR, Nittrouer CA, Guyot JL. 2003. Episodic sediment accumulation on Amazonian floodplains influenced by El Niño/Southern Oscillation. *Nature* **425**, pp. 493-497. Doi: 10.1038/nature02002

Aalto, R, Nittrouer, CN. 2012, 210-Pb Geochronology of Flood Events in Large Tropical River Systems, Philosophical Transactions of the Royal Society A, v. 370, p. 2040-2074.

Ashley, GH, 1933. The scenery of Pennsylvania – Its origin and Development based on recent studies of physiographic and glacial history. Department of Internal Affairs. Harriburg, PA. 91 pp.

Bacon AR, Richter DdeB, Bierman PR, Rood DH. 2012. Coupling meteoric ^{10}Be with pedogenic losses of ^{9}Be to improve soil residence time estimates on an ancient North American interfluve. *Geology* **40**, 9: 847-850. DOI: 10.1130/G33449.1

Balco G. 2004. The sedimentary record of subglacial erosion beneath the Laurentide Ice Sheet. Ph.D. Thesis, University of Washington. 137 pp.

Barg E, Lal D, Pavich MJ, Caffee MW, Southon JR. 1997. Beryllium geochemistry in soils: evaluation of $^{10}Be/^{9}Be$ ratios in authigenic minerals as a basis for age models. *Chemical Geology* **140**: 237-258.

Barnes JH, Sevon WD. 2002. The Geological Story of Pennsylvania (3rd Edition): Pennsylvania Geological Survey, 4th ser., Educational Series 4, 44p.

Belmont P, Gran KB, Schottler SP, Wilcock PR, Day SS, Jennings C, Lauer JW, Viparelli E, Willenbring JK, Engstrom DR, Parker G. 2011. Large Shift in Source Fine Sediment in the Upper Mississippi River. *Environ. Sci. Technol. Lett.* **45**: 8804-8810. Dx.doi.org/10.1021/es2019109

BLACKMER GC, 2005. Preliminary bedrock geologic map of a portion of the Wilmington 30- by 60-minute quadrangle, southeastern Pennsylvania: Pennsylvania

Geological Survey, 4th ser., *Open-File Report* OFBM 05–01.0, 16 pp., Portable Document Format (PDF) file.

Blakemore LC, Searle PL, Daly BK. 1987. Methods for Chemical Analysis of Soils. New Zealand Soil Bureau Report 80.

Bonczik M, 2013. A determination of the concentration level of leas 210Pb Isotope in solid samples for the assessment of radiation risk occurring in coal mines. *Journal of Sustainable mining* 12,2,1-7. https://doi.org/10.7424/jsm130201

Brantley SL, Eissenstat DM, Marshall JA, Godsey SE, Balogh-Brunstad Z, Karwan DL, Papuga SA, Roering J, Dawson TE, Evaristo J, Chadwick O, McDonnell JJ, Weathers KC 2017. Reviews and syntheses: on the roles trees play in buildung and plumbing critical zone. *Biogeosciences* 14: 5115-5142. https://doi.org/10.5194/bg-14-5115-2017

Braun DD 2004. The glaciation of Pennsylvania, USA. Developments in Quaternary Sciences **2**: 237-242. https://doi.org/10.1016/S1571-0866(04)80201-X

Brown L, Pavich MJ, Hickman RE, Klein J, Middleton R. 1988. Erosion of the eastern United States observed with ^{10}Be. *Earth Surface Processes and Landforms* **13**: 441-457.

Chmeleff J, von Blanckenburg F, Kossert K, Jacob D. 2009. Determination of the ^{10}Be half-life by multicollector ICP-MS and liquid scintillation counting. *Nuclear Instruments and Methods B* **268**, 2: 192-199. DOI: 10.1016/j.nimb.2009.09.012

Ciolkosz EJ, Waltman WJ, Simpson TW, Dobos RR. 1989. Distribution and Genesis of the Northeastern United States. *Geomorphology* **2**: 285-302.

Clark GM. 1968. Sorted Patterned Ground: New Appalachian Localities South of the Glacial Border. *Science* **161**: 355-356.

Clark GM, Ciolkosz EJ. 1988. Periglacial Geomorphology of the Appalachian highlands and interior highlands south of the glacial border – A review. *Geomorphology* **1**: 191-220.

Cogbill CV, White PS, 1991. The latitude-elevation relationship for spruce-fir forest and treeline along the Appalachian mountain chain. Vegetatio **94**: 153. https://doi.org/10.1007/BF00032629

Dannhaus N, Wittmann H, Krám P, Christl M, von Blanckenburg F, 2017. Catchment-wide weathering and erosion of mafic, ultramafic, and granite rock from cosmogenic ^{10}Be/ ^{9}Be ratios. *Geochimica et Cosmochimica Acta* **222**: 618-641. https://doi.org/10.1016/j.gca.2017.11.005

Davies BE. 1992. Inter-relationships between soil properties and the uptake of cadmium, copper, lead and zinc from contaminated softs radish (Raphanus sativus L.). *Water, Air, and Soil Pollution* **63**, pp. 331-342.

Degens ET, Williams EG, Keith ML, 1957. Environmental studies of Carboniferous sediments part I: Geochemical criteria for differentiating marine and fresh water shales. *American Association of Petroleum Geologists Bulletin* **41**: 2427–2455.

Ebert K, Willenbring J, Norton KP, Hall A, Hättestrand C. 2012. Meteoric ^{10}Be concentrations from saprolite and till in northern Sweden: Implications for glacial erosion and age. *Quaternary Geochronology* **12**: 11-22. DOI: 10.1016/j.quageo.2012.05.005

Egli M, Brandová D, Böhlert R, Filippo F, Kubik PW. 2010. ^{10}Be inventories in Alpine soils and their potential for dating land surfaces. *Geomorphology* **119**, 1-2: 62-73. Available at: http://linkinghub.elsevier.com/retrieve/pii/S0169555X10000887 [Accessed July 21, 2011].

Field CV, Schmidt GA, Koch D, Salyk C. 2006. Modeling production and climate-related impacts on ^{10}Be concentration in ice cores. *Journal of Geophysical Research* **111**, D15107. 13pp. Doi: 10.1029/2005JD006410

Fifield LK, Wasson RJ, Pillans B, Stone JOH. 2010. The longevity of hillslope soil in SE and NW Australia. Catena **81**: 32-42. DOI: 10.1016/j.catena.2010.01.003

Frank M, Schwarz B, Baumann S, Kubik PW, Suter M, Mangini A. 1997. A 200 kyr record of cosmogenic radionuclide production rate and geomagnetic field intensity from ^{10}Be in globally stacked deep-sea sediments. *Earth and Planetary Science Letters* **149**: 121-129.

Goodbred SL, Kuehl SA. 1998. Floodplain processes in the Bengal Basin and the storage of Ganges-Brahmaputra river sediment: an accretion study using Cs-137 and Pb-210 geochronology. *Sedimentary Geology* **121**, pp. 239-258. Doi: 10.1016/S0037-0738(98)00083-7

Graly JA, Bierman PR, Reusser LJ, Pavich MJ. 2010. Meteoric ^{10}Be in soil profiles – A global meta-analysis. *Geochim, Cosmochim. Acta* **74**: 6814-6829. DOI: 10.1016/j.gca.2010.08.036

Graly JA, Reusser LJ, Bierman PR. 2011. Short and long-term delivery rates of meteoric ^{10}Be to terrestrial soils. *Earth and Planetary Science Letters* **302**: 329-336. DOI: 10.1016/j.epsl.2010.12.020

Hack JT. 1982. Physiographic divisions and differential uplift in the Piedmont and Blue Ridge. 49 pp.

He Q, Walling DE. 1997. The distribution of fallout ^{137}Cs and ^{210}Pb in undisturbed and cultivated soils. *Applied Radiation Isotopes* **48**, 5: 677-690. PII: S0969-8043(96)00302-8

Heikkilä U, Beer J, Feichter J. 2007. Modeling of the atmospheric transport of the cosmogenic radionuclides ^{10}Be and ^{7}Be using the ECHAM5-HAM General Circulation Models. *Atmospheric Chemistry and Physics* **8**, pp. 2797-2809.

Jungers MC, Bierman PR, Matmon A, Nichols K, Larsen J, Finkel R. 2009. Tracing hillslope sediment production and transport with in situ and meteoric ^{10}Be. *Journal of*

Geophysical Research **114**(F4): 1-16. Available at: http://www.agu.org/pubs/crossref/2009/2008JF001086.shtml [Accessed July 21, 2011].

Korschinek G, Bergmaier A, Faestermann T, Gerstmann UC, Knie K, Rugel G, Walner A, Dillmann I, Dollinger G, von Gostomski CL, Kossert K, Maiti M, Poutivtsev M, Remmert A. 2010. A new value for the half-life of ^{10}Be by Heavy-Ion Elastic Recoil Detection and liquid scintillation counting. *Nuclear Instruments and Methods in Physics Research B* **268**: 187-191. DOI: 10.1016/j.nimb.2009.09.020

Lal R, Fifield LK, Tims RJ, Wasson RJ, Howe D. 2012. A study of soil formation using ^{10}Be in wet-dry tropics of northern Australia. *EPJ Web of conferences* **35**, 01001. DOI: 10.1051/epjconf/20123501001

Larsen IJ, Almond PC, Eger A, Stone JO, Montgomery DR, Malcolm B. 2014. Rapid soil production and weathering in the southern Alps, New Zealand. Science 343: 637-640. DOI: 10.1126/science.1244908

Leser H. 1977. Feld- und Labormethoden der Geomorphologie. Berlin (de Gruyter).

Ma L, Chabaux F, West N, Kirby E, Jin L, Brantley S. 2013. Regolith production and transport in the Susquehanna Shale Hills Critical Zone Observatory, Part 1: Insights from U-series isotopes. *Journal of Geophysical Research: Earth Surface* **118**: 722-740. DOI: 10.1002/jgrf.20037

Mabit L, Benmansour M, Walling DE. 2008. Comparative advantages and limitations of the fallout radionuclides ^{137}Cs, $^{210}Pb_{ex}$ and ^{7}Be for assessing soil erosion and sedimentation. *Journal of Environmental Radioactivity* **99**, 12, pp. 1799-1807. http://www.ncbi.nlm.nih.gov/pubmed/18947911

Matsuoka N. 2001. Solifluction rates, processes and landforms: a global review. *Earth Science Reviews* **55**: 107-134. PII:S0012-8252(01)00057-5

Nelson KJP, Nelson FE, Walegur MT 2007. Periglacial Appalachia: paleoclimate significance of blockfield elevation gradients, eastern USA. *Permafrost and Periglacial Processes* **18**: 61-73. DOI: 10.1002/ppp.574

Newbold JD, Bott TL, Kaplan LA, Sweeney BW, Vanotte RL. 1997. Organic matter dynamics in White Clay Creek Pennsylvania, USA. *Stream Organic Matter Budgets* **16**: 46-50.

Pavich, M.J., Brown L, Valette-Silver JN, Klein J, Middleton R. 1985. ^{10}Be analysis of a Quaternary weathering profile in the Virginia Piedmont. *Geology* **13**: 39-41. DOI: 10.1130/0091-7613(1985)13<39:BAOAQW>2.0.CO;2

Perreault LM, Yager EM, Aalto R: 2012. Application of $^{210}Pb_{ex}$ inventories to measure net hillslope erosion at burned sites. *Earth Surface Processes and Landforms* **38**, 2, pp. 133-145. Doi: 10.1002/esp.3266.

Persson BRR, Holm E. 2011. Polonium-210 and lead-210 in the terrestrial environment: A historical review. *Journal of Environmental Radioactivity* **102**, 5, pp. 420-429. http://ww.ncbi.nlm.nih.gov/pubmed/21377252

Resner K, Kyungsoo Y, Hale C, Aufdenkampe A, Blum A, Sebestyen S. 2011. Elemental and mineralogical changes in soils due to bioturbation along on earthworm invasion chronosequence in Northern Minnesota. *Applied Geochemistry* **26**, S127-S131. http://dx.doi.org/10.1016/j.apgeochem.2011.03.047

Reusser L, Bierman P, Rood D. 2015. Quantifying human impacts on rates of erosion and sediment transport at a landscape scale. *Geology* G36272.1, first published on January 7, 2015. DOI: 10.1130/G36272.1

Schaller M, von Blanckenburg F, Veldkamp A, Tebbens LA, Hovius N, Kubik PW. 2002. A 30,000 yr record of erosion rates from cosmogenic ^{10}Be in Middle European river terraces. *Earth and Planetary Science Letters* **204**: 307-320. PII: S0012-821X(02)00951-2

Scheffer F, Schachtschabel P, 2010. *Lehrbuch der Bodenkunde, 16. Auflage*, Spektrum, Akademischer Verlag, Heidelberg, 570 pp.

Schoonejans J, Vanacker V, Opfergelt S, Christl M. Long-term soil erosion derived from in-situ ^{10}Be and inventories of meteoric ^{10}Be in deeply weathered soils in southern Brazil. *Chemical Geology* **466**: 380-388. http://dx.doi.org/10.1016/j.chemgeo.2017.06.025

Sevon WD. 2000. Physiographic Provinces of Pennsylvania, Map 13. Pennsylvania Geologic Survey. Harrisburg PA.

Sevon D, Braun D. 2000. Glacial Deposits of Pennsylvania. Bureau of Topographic and Geologic Survey, Pennsylvania. Department of Conservation and Natural Resources.

Simms DL. 1988. Lead in softs: A European's view, in Issues and Guidelines. Be Davies and BG Wixson (Eds), Lead in Soft., *Science Reviews Limited, Northwood*, pp. 27-47.

Stanford SD, Seidl MA, Ashley GM. 2000. Exposure age and erosional history of an upland planation surface in the US Atlantic Piedmont. *Earth Surface Processes and Landforms* **25**: 939-950.

Stone JOH. 1998. A rapid fusion method for separation of beryllium-10 from soils and silicates. *Geochimica et Cosmochimica Acta* **62**(3): 555-561.

Vance D, Bickle M, Ivy-Ochs S, Kubik PW. 2003. Erosion and exhumation in the Himalaya from cosmogenic isotope inventories of river sediments. *Earth and Planetary Science Letters* **206**: 273-288. DOI: 10.1016/S0012-821X(02)01102-0

Waroszewski J, Egli M, Brandová D, Christl M, Kabala C, Malkiewicz M, Kierczak J, Glina B, Jezierski P. Identifying slope processes over time and their imprint in soils of medium-high mountains of Central Europe (the Karkonosze Mountains, Poland). *Earth Surface Processes and Landforms*. DOI: 10.1002/esp.4305

West N, Kirby E, Bierman P, Slingerland R, Ma L, Rood D, Brantley S. 2013. Regolith production and transport at the Susquehanna Shale Hills Critical Zone Observatory, Part 2: Insights from meteoric ^{10}Be. *J. Geophys. Res.: Earth Surface* **118**: 1877-1896. DOI: 10.1002/jgrf.20121

West N, Kirby E, Bierman P, Clarke BA. 2014. Aspect-dependent in regolith creep revealed meteoric ^{10}Be. *Geology* **42**: 507-510. DOI: 10.1130/G35357.1

Willenbring JK, von Blanckenburg F. 2010. Meteoric cosmogenic beryllium-10 adsorbed to river sediment and soil: Applications for Earth-surface dynamics. *Earth Science* Reviews **98**, 1-2: 105-122. Available at: http://linkinghub.elsevier.com/retrieve/pii/S0012825209001639 [Accessed August 19, 2011].

Zepp H. 2011. Geomorphologie – Eine Einfuehrung. 5. Auflage. Ferdinand Schoening Verlag, Paderborn.

Tables

Table 1 – Slope analysis for the five sample points Wy-Wood, Bluebell, Penn Oak, Ag-Field and Weather Station, measured within a 10 m radius of the elevation profiles displayed in Figure 2C using Arc GIS tools.

Profile name	**Wy-Wood**	**Bluebell**	**Penn Oak**	**Ag-Field**	**Weather Station**
Min [deg]	1	2	1	5	1
Max [deg]	4	9	6	11	7
Average [deg]	3	5	4	8	3

Table 2 – ^{10}Be analysis for the hilltop (a) and valley hollow (b) profiles. ^{10}Be inventory is calculated using Equation 1 and includes soil density that was calculated for each interval with the help of sample weight and sampling tube dimensions. The timing of accumulation is determined according to Equation 2. Time of accumulation cannot be calculated for the valley hollow profiles as discussed in the text. There are no pH measurements for the Penn Oak profile. The pH measurements for the Weather Station and Blue Meadow profile are based on the depth intervals 10-20, 20-30, 30-40, 40-50, and 60 -70 cm.

	Depth Intervall [cm]	^{10}Be [$*10^8$ g^{-1}]	Clay [%]	Density [g/cm^3]	pH DI water	pH $CaCl_2$	^{10}Be Accumulative over depth [10^{10} atoms cm^{-2}]	Age [kyr]
Penn-Oak	10 - 12	3.74 ±0.012	18	1.4			0.59 ±0.01	5 ±0.06
	20 - 22	3.79 ±0.016	20	1.5			1.14 ±0.02	10 ±0.13
	30 - 32	3.98 ±0.013	33	1.8			1.77 ±0.02	15 ±0.21
	40 - 42	3.03 ±0.012	22	1.7			2.39 ±0.03	20 ±0.27
	60 - 62	4.65 ±0.019	27	1.8			3.73 ±0.05	31 ±0.45
	100 - 102	1.32 ±0.016	14	1.4			5.59 ±0.09	47 ±0.74
	140 - 142	0.51 ±0.015	10	1.4			6.09 ±0.10	51 ±0.80
	200 - 202	0.21 ±0.026	9	1.9			6.44 ±0.10	54 ±0.86
	248 - 250	0.12 ±0.033	10	1.9			6.59 ±0.11	56 ±0.89
	300 - 302	0.15 ±0.036	12	1.4			6.70 ±0.11	57 ±0.92
Weather station	10 - 12	5.02 ±0.015	32	1.4	5.5	4.8	0.76 ±0.01	6 ±0.09

20 - 22	3.36 ±0.016	40	1.6	4.9	4.2	1.39 ±0.02	12 ±0.17
30 - 32	2.75 ±0.017	37	1.6	4.6	4	1.89 ±0.03	16 ±0.24
40 - 42	1.06 ±0.016	18	1.5	4.8	4.2	2.19 ±0.03	18 ±0.28
68 - 70	0.82 ±0.015	12	1.5	4.9	4.1	2.58 ±0.04	22 ±0.33
100 - 102	0.34 ±0.025	6	1.6			2.86 ±0.04	24 ±0.37
140 - 142	0.13 ±0.033	7	1.5			3.01 ±0.05	25 ±0.41
200 - 202	0.01 ±0.176	5	1.8			3.08 ±0.05	26 ±0.43
270 - 272	0 ±0.010	9	1.5			3.08 ±0.05	-

	Depth Intervall	^{10}Be	Clay	Density	pH		^{10}Be without initial	^{10}Be Accumulative inventory of sediment packages	Age of sediment packages
	[cm]	[*10^8 g^{-1}]	[%]	[g/cm^3]	DI water	$CaCl_2$	[*10^8 g^{-1}]	[*10^{10} atoms cm^{-2}]	[kyr]
Blue	10 - 12	7.84 ±0.018	22	1.1	4.2	3.8	3.00	0.36 ±0.02	
Meadow	20 - 22	7.37 ±0.016	22	1.3	4.3	3.9	2.53	0.69 ±0.03	
	30 - 32	7.00 ±0.012	24	1.5	4.0	3.8	2.16	1.03 ±0.05	
	40 - 42	8.42 ±0.019	26	1.7	4.3	3.9	3.59	1.49 ±0.07	12 ±0.57
	60 - 62	14.23 ±0.014	38	1.5	4.4	4.0	9.40	2.03 ±0.06	
	120 - 122	5.68 ±0.012	41	1.8			0.84	7.08 ±0.19	
	200 - 202	4.12 ±0.012	34	1.8			0	7.68 ±0.09	65 ±0.72
	294 - 296	10.96 ±0.013	33	1.3			6.12	7.65 ±0.14	65 ±1.15
Wy-Wood	18 - 20	9.33 ±0.012	26	1.1	4.2	3.7	4.49	0.95 ±0.02	
	40 - 42	7.50 ±0.020	41	1.6	4.2	3.7	2.67	1.99 ±0.06	
	71 - 73	6.35 ±0.012	25	1.8	4.1	3.7	1.51	3.08 ±0.12	
	101 - 117	5.41 ±0.023	33	1.8	4.2	3.9	0.57	3.77 ±0.19	
	133 - 148	5.74 ±0.016	32	1.8	4.4	3.9	0.90	4.19 ±0.25	
	164 - 180	6.29 ±0.012	26	1.8	4.5	4.1	1.46	4.86 ±0.30	41 ±2.50
	189 - 204	7.97 ±0.025	22	1.8	5.2	4.3	3.13	1.38 ±0.06	12 ±0.51
Ag-field	18 - 28	11.35 ±0.017	30	1.6	6.5	6.4	6.51	2.33 ±0.07	
	53 - 60	8.61 ±0.012	29	1.4	6.6	6.2	3.77	4.84 ±0.15	
	70 - 78	7.40 ±0.012	30	1.5	6.6	6.1	2.57	5.64 ±0.17	48 ±1.41
	95 - 110	9.98 ±0.024	20	1.8	6.5	6.0	5.14	1.82 ±0.08	
	155 - 170	10.91 ±0.016	18	1.8	6.7	6.0	6.08	7.88 ±0.30	67 ±2.50
	205 - 215	11.50 ±0.012	16	1.8	6.0	5.1	6.66	5.45 ±0.13	
	247 - 251	8.81 ±0.014	14	1.8	5.3	5.0	3.97	9.18 ±0.23	78 ±1.90

Figures

Figure 1 – The Commonwealth of Pennsylvania and its six main physiographic provinces in relation to the Christina River Basin (CRB). Glacial advances within Pennsylvania are indicated by coloured lines: Wisconsinan (purple), Late Illinoian (green), Pre-Illinoian (orange) (Adapted from Sevon (2000) and Sevon and Braun (2000)).

Figure 2 – (A) The Christina River Basin and its four sub-basins: Christina River (CR), Brandywine Creek (BC), Red Clay Creek (RCC) and White Clay Creek (WCC). The sample sites are mainly from the north-west of WCC but the Bluebell Meadow site is located near to the drainage divide to RCC. (B) A hillshade created from a DEM showing the study area (1 m resolution LIDAR), including the sample sites. The white lines mark the transects shown as topographic profiles in (C). The transects show the relevant topographic features of each sample site (black point), which are usually perpendicular to the strike of the hills.

Figure 3 – (A) ^{10}Be concentration with depth in the **Penn Oak** profile including the percentage of clay. The age model is displayed to the right of the profile. The ^{10}Be concentration and clay distribution with depth in the **Weather Station** profile is shown in (B), also including the age model.

Figure 4 –^{10}Be, clay and element concentration (Fe_2O_3, Al_2O_3) with depth in the **Bluebell Meadow profile**. The age model on the right is based on the ^{10}Be measurements, where inherited ^{10}Be (dashed grey line) is deducted. Rippled grey lines mark areas with a change in sediment deposition and the dashed grey line marks the ^{10}Be concentration delivered to the site with the sediment and not by

atmospheric fallout (see text for further information). Note that samples from below 100 cm were collected from material in a fissure in otherwise hard bedrock, and the sample at 60 cm may reflect illuviation on top of that bedrock.

Figure 5 – ^{10}Be, clay and element concentration (Fe_2O_3, Al_2O_3) with depth in the **Ag-Field (**A). There are no Fe_2O_3 and Al_2O_3 measurement for the **Wy-Wood** profile **(**B) The age models on the right of each profile are based on the ^{10}Be measurements (inherited ^{10}Be (dashed grey line) is deducted). Rippled grey lines mark areas with a change in sediment deposition and the dashed grey line marks the ^{10}Be concentration delivered to the site with the sediment and not by atmospheric fallout (see text for further information).

Figure 6 (A) Bluebell Meadow: This profile displays an undisturbed ^{210}Pb distribution with depth, with high concentrations at the top and a gradual decrease with depths, hence there was no major soil disturbance within the last 100 years. (B) Penn Oak: This profile shows an increase in ^{210}Pb activity at 10 cm of depth and therefore soil disturbance within the last 100 years is expected. This agrees with historical records, which consider that sediment was added to the site to protect the roots of the oak tree nearby. (C) Wy-Wood: No major sediment redistribution occurred within this sample site, this is inferred because of the undisturbed ^{210}Pb distribution with depth (high concentration at the top with a gradual decrease with depths). (D) Weather Station: This profile has an undisturbed ^{210}Pb distribution with depth but a much lower ^{210}Pb activity compared to the other ^{210}Pb profiles. (E) Ag-field: ^{210}Pb activity in this profile is substantially disturbed within the first 40 cm due to soil loosening.

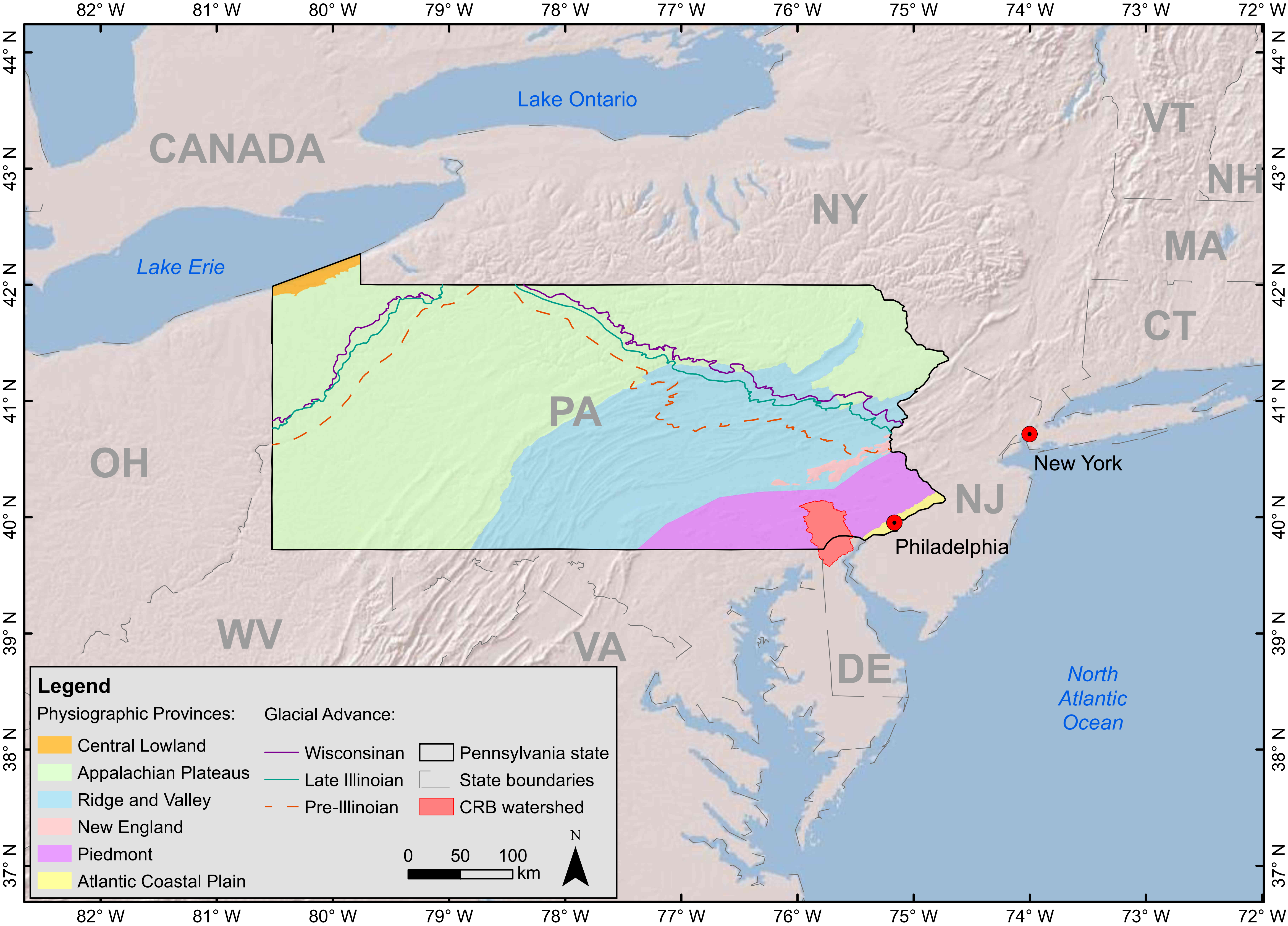

82° W
81° W
80° W
79° W
78° W
77° W
76° W
75° W
74° W
73° W
72° W
44° N
43° N
42° N
41° N
40° N
39° N
38° N
37° N
Lake Ontario
CANADA
VT
NH
NY
MA
Lake Erie
CT
PA
OH
New York
NJ
Philadelphia
WV
VA
DE
North Atlantic Ocean
Legend
Physiographic Provinces:
Central Lowland
Appalachian Plateaus
Ridge and Valley
New England
Piedmont
Atlantic Coastal Plain
Glacial Advance:
Wisconsinan
Late Illinoian
Pre-Illinoian
Pennsylvania state
State boundaries
CRB watershed
0 50 100
km
N

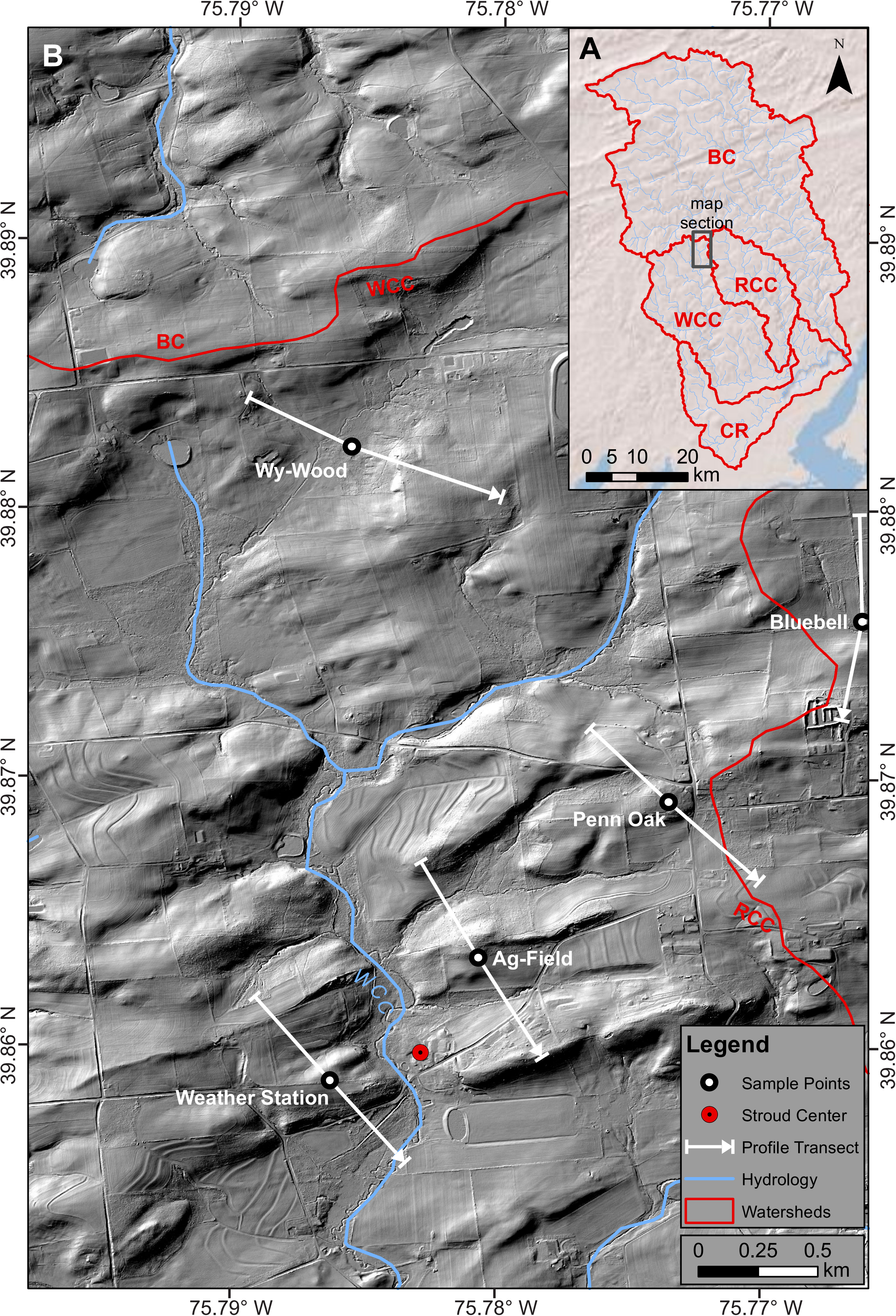
75.79° W
75.78° W
75.77° W
39.89° N
39.88° N
39.87° N
39.86° N
B
A
N
BC
map section
RCC
WCC
CR
0 5 10 20
km
WCC
BC
Wy-Wood
Bluebell
Penn Oak
RCC
Ag-Field
WCC
Weather Station
Legend
Sample Points
Stroud Center
Profile Transect
Hydrology
Watersheds
0 0.25 0.5
km

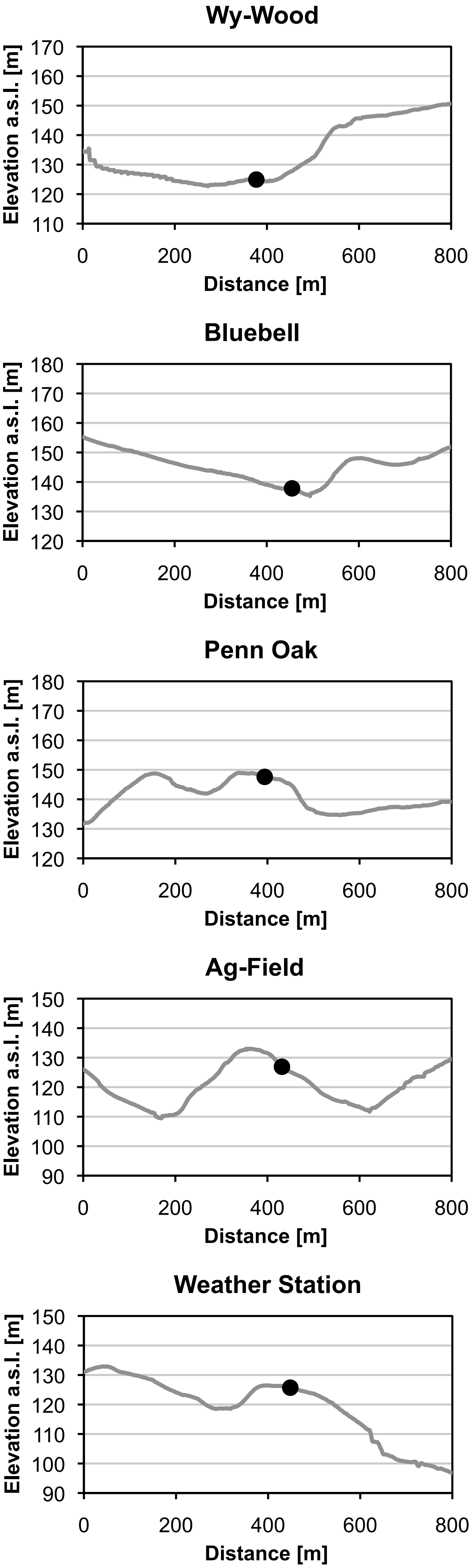

Wy-Wood
Elevation a.s.l. [m]
170
160
150
140
130
120
110
0
200
400
600
800
Distance [m]
Bluebell
Elevation a.s.l. [m]
180
170
160
150
140
130
120
0
200
400
600
800
Distance [m]
Penn Oak
Elevation a.s.l. [m]
180
170
160
150
140
130
120
0
200
400
600
800
Distance [m]
Ag-Field
Elevation a.s.l. [m]
150
140
130
120
110
100
90
0
200
400
600
800
Distance [m]
Weather Station
Elevation a.s.l. [m]
150
140
130
120
110
100
90
0
200
400
600
800
Distance [m]

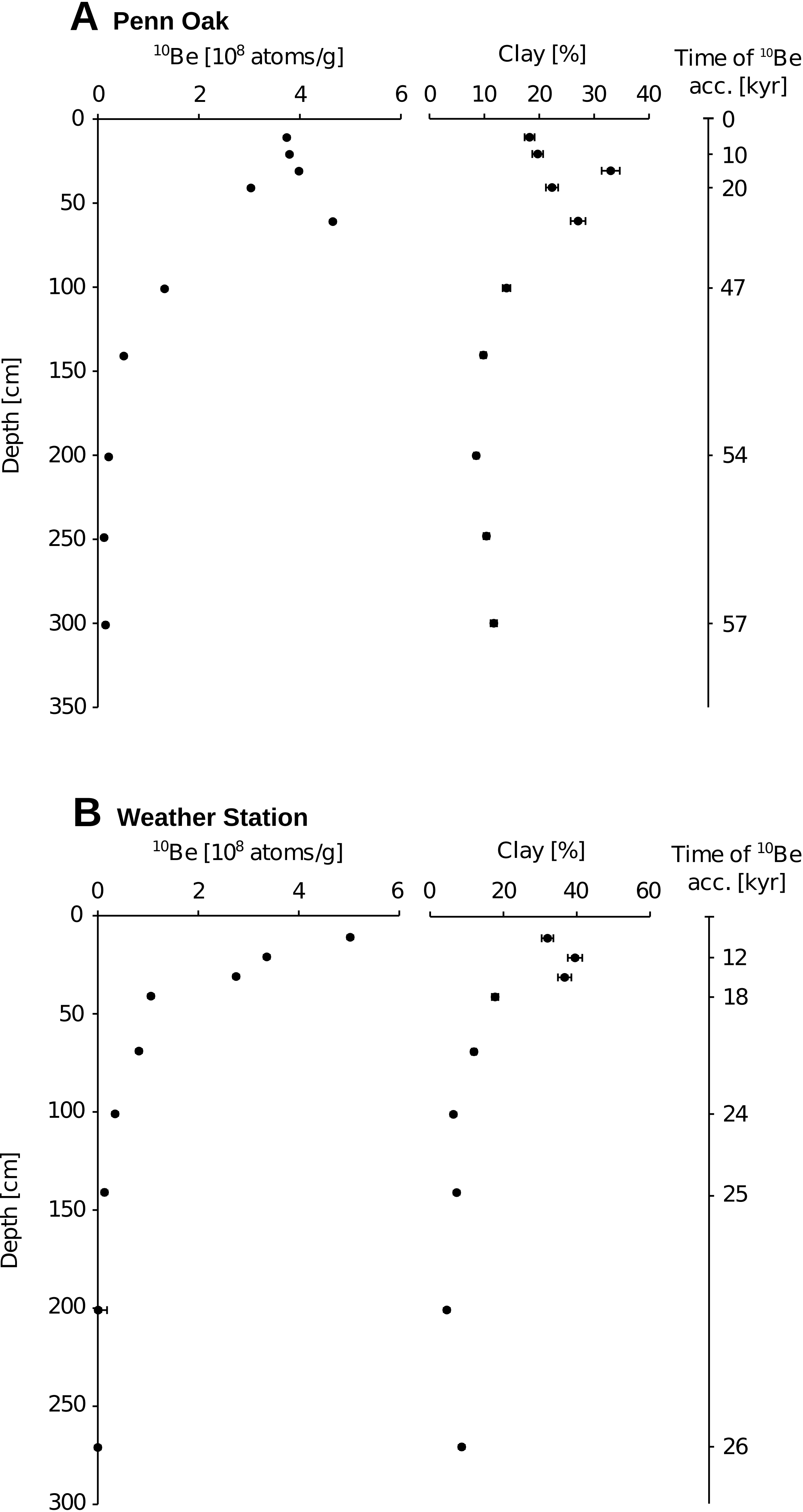
A Penn Oak
^{10}Be [10^8 atoms/g]
Clay [%]
Time of ^{10}Be acc. [kyr]
Depth [cm]
0 10 20 47 54 57
B Weather Station
^{10}Be [10^8 atoms/g]
Clay [%]
Time of ^{10}Be acc. [kyr]
Depth [cm]
12 18 24 25 26

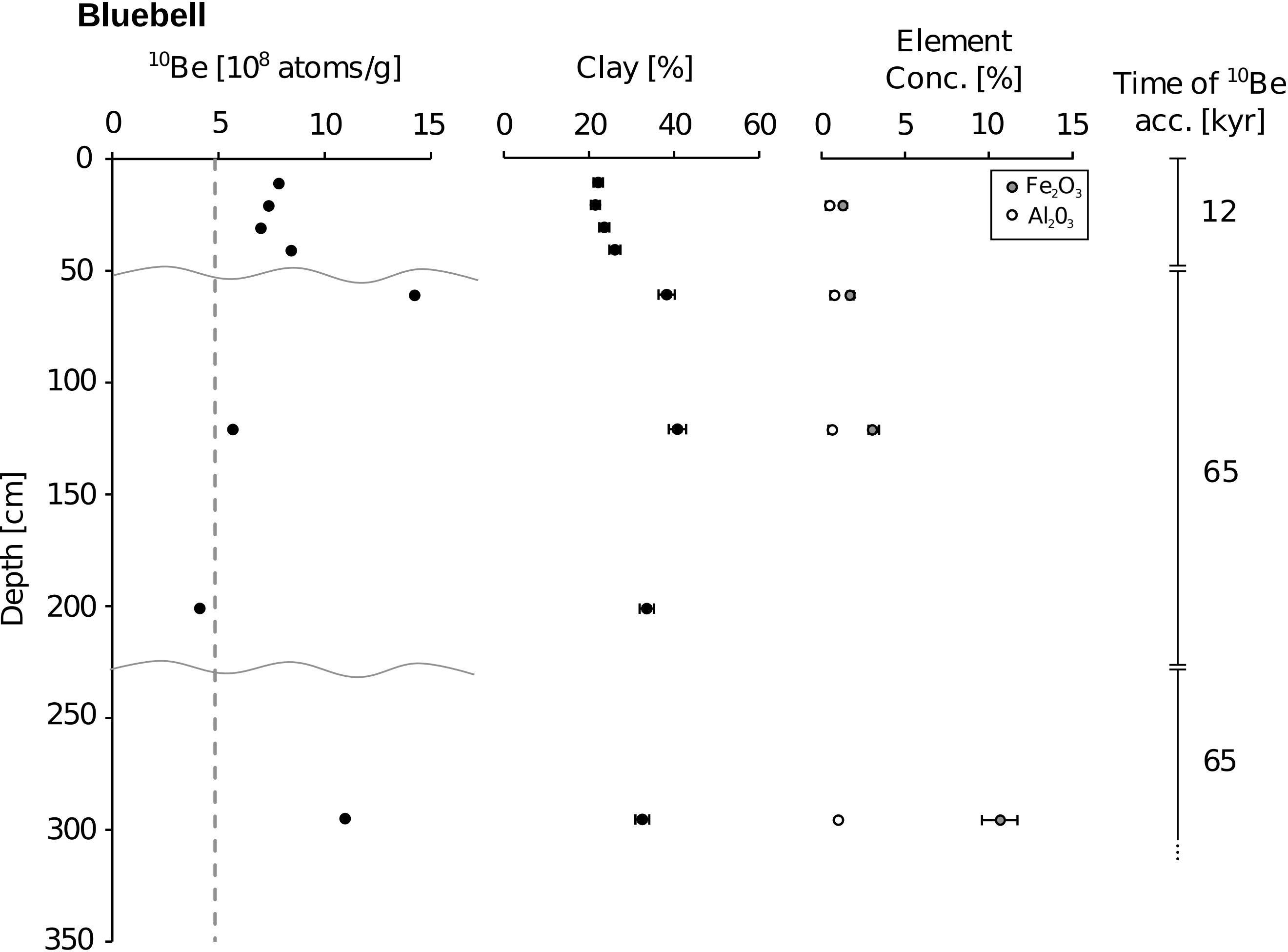

Bluebell
10Be [10^8 atoms/g]
0
5
10
15
Clay [%]
0
20
40
60
Element
Conc. [%]
0
5
10
15
Fe2O3
Al2O3
Time of 10Be
acc. [kyr]
12
65
65
Depth [cm]
0
50
100
150
200
250
300
350

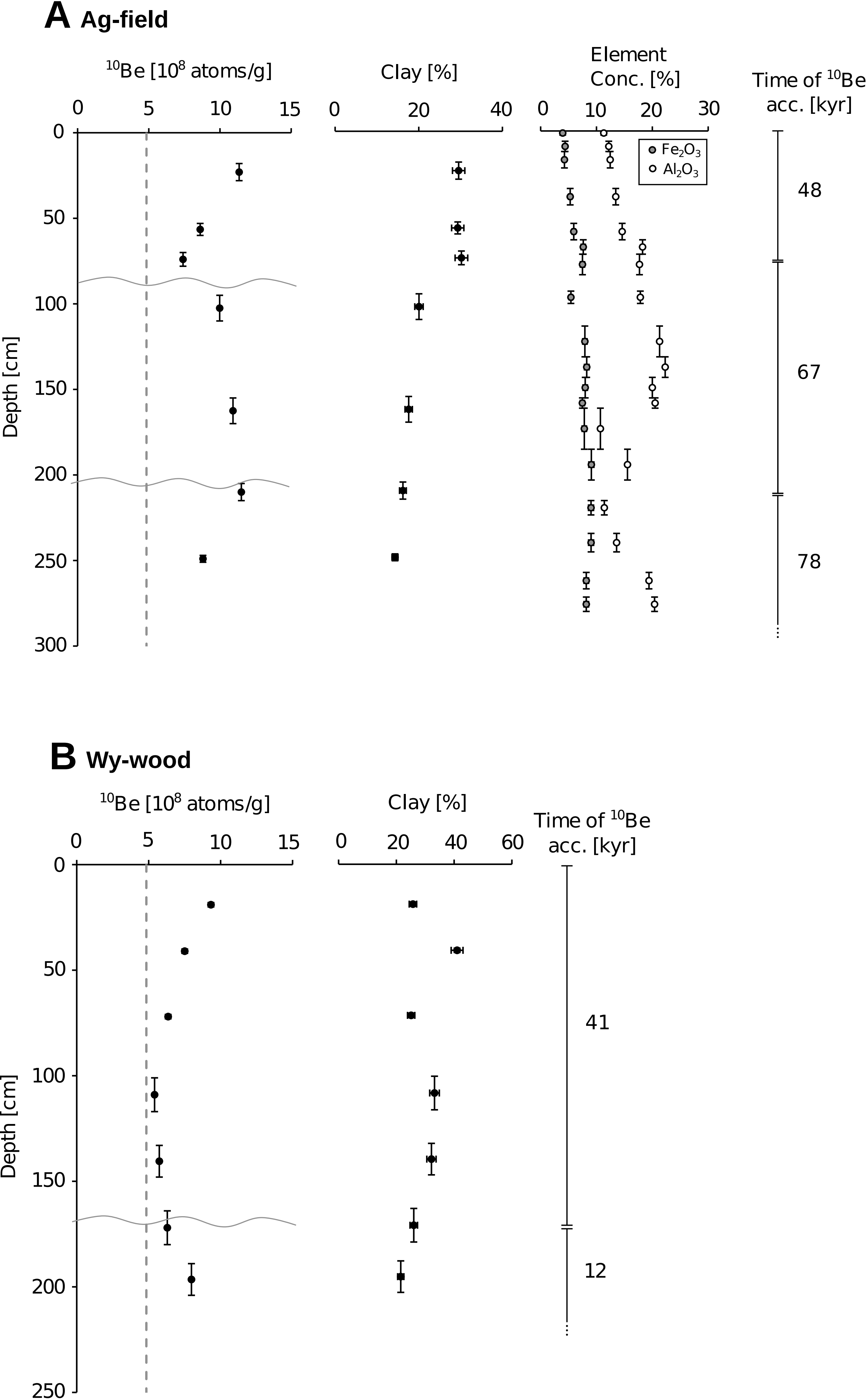

A Ag-field
^{10}Be [10^8 atoms/g]
Clay [%]
Element Conc. [%]
Time of ^{10}Be acc. [kyr]
Fe_2O_3
Al_2O_3
Depth [cm]
48
67
78
B Wy-wood
^{10}Be [10^8 atoms/g]
Clay [%]
Time of ^{10}Be acc. [kyr]
Depth [cm]
41
12

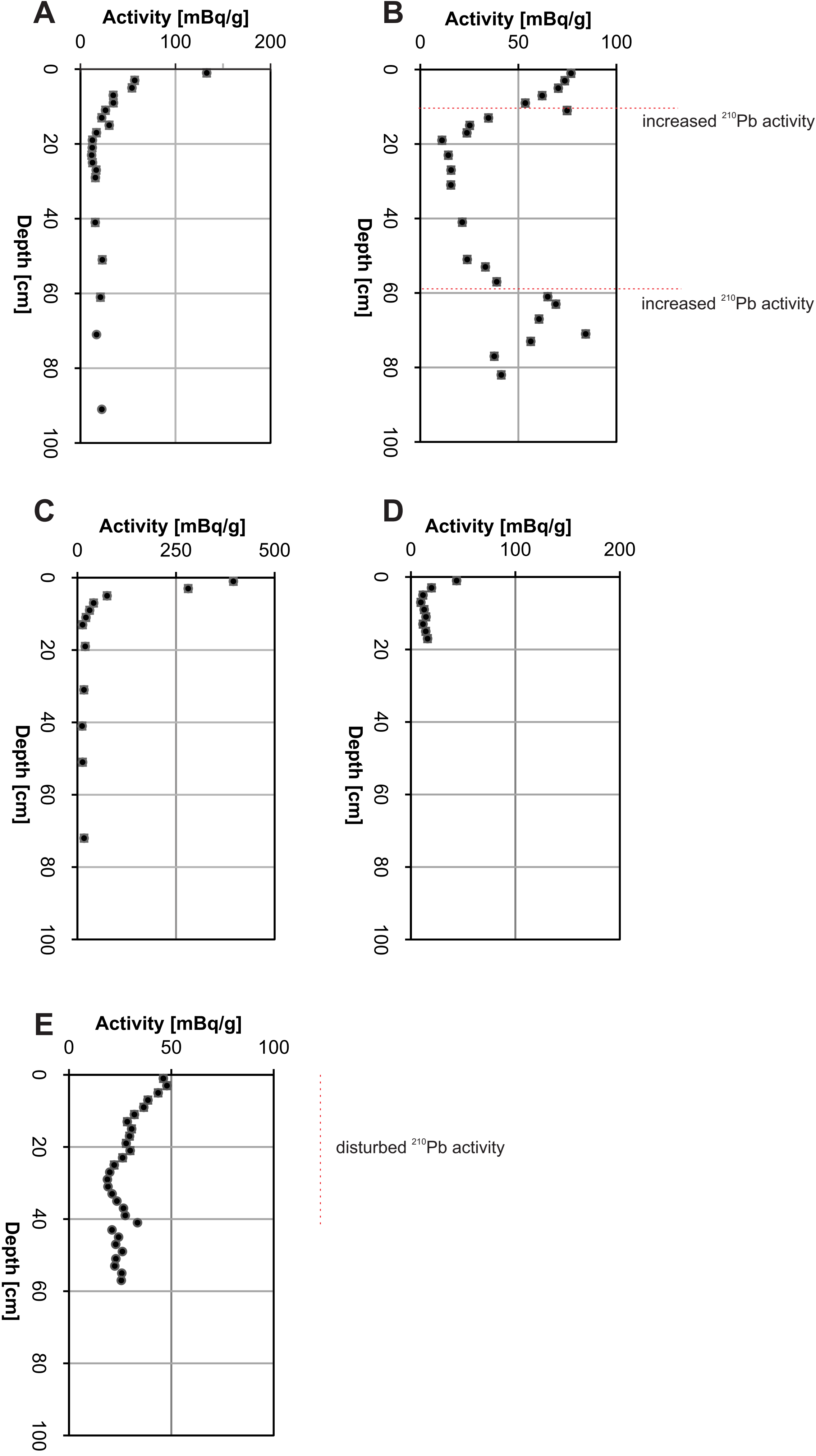

A
Activity [mBq/g]
0
100
200
0
20
40
60
80
100
Depth [cm]
B
Activity [mBq/g]
0
50
100
increased 210Pb activity
increased 210Pb activity
C
Activity [mBq/g]
0
250
500
D
Activity [mBq/g]
0
100
200
E
Activity [mBq/g]
0
50
100
disturbed 210Pb activity